Vaccine 37 (2019) 2857–2863

Contents lists available at ScienceDirect

Vaccine

journal homepage: www.elsevier.com/locate/vaccine

Attenuation of a dengue virus replicon by codon deoptimization of nonstructural genes

Gayathri Manokaran [a,b,1], Sujatmoko [a,1], Kirsty Grace McPherson [a], Cameron Paul Simmons [a,b,c,*]

[a] Department of Microbiology and Immunology, Peter Doherty Institute for Infection and Immunity, University of Melbourne, Parkville, Victoria, Australia
[b] Institute of Vector Borne Disease, Monash University, Clayton, Victoria, Australia
[c] Oxford University Clinical Research Unit, Wellcome Trust Major Overseas Programme, District 5, Ho Chi Minh City, Viet Nam

ARTICLE INFO

Article history:
Received 8 January 2019
Received in revised form 15 March 2019
Accepted 17 March 2019
Available online 15 April 2019

Keywords:
Dengue
Codon deoptimization
Replicon
Vaccine
Attenuation

ABSTRACT

The overwhelming increase of dengue virus (DENV) infections in recent years shows that current strategies to combat dengue do not work. The lack of a highly effective dengue vaccine and the limited effectivity of vector controls exacerbate this situation. To point the way to a novel method of creating DENV vaccine candidates, here we disrupted the codon usage in a DENV-2 reporter replicon to generate variants with different replication characteristics. Six different mutated constructs containing stretches of altered codon usage in the non-structural genes were generated. The mutated sequences were deoptimized to the least favorable codons for human cells. We studied the replication efficiency of these constructs by measuring luciferase reporter activity, relative RNA fold change, and NS1 secretion. Our findings showed that the level of virus attenuation is closely associated with the amount of codon deoptimization. Indeed, replication was completely abolished in extensively-deoptimized constructs D2Rep-6 and D2Rep-5, intermediate with constructs D2Rep-4 (771 bp silent mutations) and D2Rep-3 (756 bp silent mutations) and restored almost to wildtype levels with constructs D2Rep-2 (394 silent mutations) and D2Rep-1 (48 silent mutations). We also determined that the position of codon deoptimization within the genome is crucial to the degree of attenuation observed. Based on our analysis, we propose that the design for an ideal DENV vaccine candidate could include 700–1500 silent mutations within the NS2A and NS3 genes. Our results suggest that codon deoptimization is an ideal strategy that can readily be used to develop a DENV vaccine candidate with "fine-tuned" attenuation.

1. Introduction

Mosquito-borne *Flaviviruses* pose an emerging global threat. Dengue viruses (DENV) cause an estimated 100 million symptomatic infections each year and are endemic in much of tropical Asia and Latin America [1]. Due to the absence of licensed antiviral drugs, treatment against dengue is restricted to supportive care and the only vaccine approved for use has limited variable efficacy and is suitable only for those who have been previously infected [2,3]. New approaches are needed in order to nurture a pipeline of dengue vaccine candidates.

There are 64 different codons in nature; 61 codons encode for the 20 different amino acids and 3 for the stop codons. The overabundance of codons results in most amino acids, except for tryptophan and methionine, to be encoded by more than one codon. Redundancy in codon usage for most amino acids has enabled codon usage bias to evolve in different species' genomes [4,5]. The genomes of arboviruses such as DENV that infect both mosquitoes and humans have evolved in a way that successfully navigates the existence of different codon usage biases in each host species [6,7]. Codon deoptimization of the viral genome involves substituting the native codons in the viral genome with the least preferred codons for the particular host organism. Likewise, some codon pairs are found in open reading frames significantly more or less frequently than expected based on the overall frequencies of the two codons that form a particular codon pair. Modifying the codon pairs to codons that are prone to pair less frequently with one another, independently of individual codon bias is known as codon pair deoptimization [8–10].

Previous studies have used both codon and codon pair deoptimization to attenuate replication of poliovirus, respiratory syncytial virus, lymphocytic choriomeningitis virus and influenza [11–14]. In DENV-2, the E, NS3 and NS5 genes in the genome were

* Corresponding author at: Institute of Vector Borne Disease, Monash University, Clayton, Victoria, Australia.
E-mail address: cameron.simmons@worldmosquito.org (C.P. Simmons).
[1] G.M. and S. contributed equally to this work.

https://doi.org/10.1016/j.vaccine.2019.03.062
0264-410X/

recoded to favour codon pair usage bias found in mosquitoes [15]. The resultant DENV viruses grew optimally in insect cells but poorly in mammalian cells [15]. Collectively, these studies provide proof of concept that codon/codon pair deoptimization can cause virus attenuation, including in DENV.

Here we disrupted the codon usage in a DENV-2 reporter replicon to provide proof of concept that this approach can be calibrated to generate variants with a range of replication characteristics and thus point the way to a method of creating DENV vaccine candidates.

2. Results

2.1. Generation of codon deoptimized reporter constructs

Using a previously well-described DENV-2 reporter replicon [16], six different mutated constructs containing stretches of altered codon usage in the non-structural genes were generated (Fig. 1A). The mutated sequences were deoptimized to the least favorable codons for human cells. The deoptimized reporter replicons all had codon adaptation indexes (CAI) [17] that were lower than the wildtype replicon (Fig. 1B) suggesting they might be less efficient templates for translation in mammalian cells.

2.2. Characteristics of reporter construct activity

Baby hamster kidney (BHK-21) cells were electroporated with RNA derived from each reporter construct so as to measure relative replication performance. Replicons with extensive codon deoptimization (D2Rep-6 and D2Rep-5) had relatively low luciferase activity suggesting limited replication (Fig. 2A and D). Only initial luciferase activity of both constructs upon electroporation was observed at 6 h post-transfection (h.p.t.) (Fig. 2A and D). Quantification of reporter-derived RNA levels from D2Rep-6 and D2Rep-5 showed a gradual increase up till 72 h.p.t., after which they dropped to similar levels as D2Rep-GDD, the replication deficient replicon. At 24 h.p.t and 96 h.p.t, we observed that the RNA levels of both constructs are significantly lower as compared to D2Rep-WT, (Fig. 2B and E). Using the DENV ELISA, we found that D2Rep-6 and D2Rep-5 did not secrete NS1 upon transfection into cells. Collectively, these data suggest that the magnitude and/or location of codon deoptimization in D2Rep-6 and D2Rep-5 dramatically reduced reporter replication.

To understand if the location of codon deoptimization affected attenuation, we next compared reporter outputs from D2Rep-4 (771 bp silent mutations in NS2A-NS3) and D2Rep-3 (756 bp silent mutations in NS3-NS4A). Both constructs had significantly higher replication as compared to GDD, but lower replication fitness than D2Rep-WT, as measured by luciferase activity and RNA levels (Fig. 3A, B, D and E). Interestingly, D2Rep-4, which had codon deoptimized NS2A-NS3, had a 1-log increase in luciferase activity compared to D2Rep-3 (codon deoptimized NS3-NS4A) at 72 and 96 h.p.t. despite having more mutations (Fig. 3A and D). Likewise, we observed that at 72 h.p.t, the RNA level of D2Rep-4 was higher than D2Rep-WT (Fig. 3B). Neither D2Rep-4 nor D2Rep-3 secreted NS1 into the supernatant (Fig. 3C and F). These findings suggest that the genomic location of codon deoptimization can also influence reporter activity.

We next examined if constructs with low numbers of deoptimized codons were attenuated. We electroporated two constructs: D2Rep-2 which carries 394 silent NS3 mutations and D2Rep-1 with 48 silent mutations. As compared to all the other constructs, significantly higher luciferase activity was seen with both D2Rep-2 and D2Rep-1 (Fig. 4A and D). As expected, D2Rep-1, the construct with the least codon deoptimization, had high levels of luciferase, with only the 24 h timepoint being significantly different from D2Rep-WT (Fig. 4D). Quantification of RNA levels showed that D2Rep-2 resulted in RNA levels similar to D2Rep-WT. Surprisingly, we observed that the RNA levels of D2Rep-1 are similar to replication-deficient D2Rep-GDD (Fig. 4E). However, the trends observed with the luciferase assay were similar to results from ELISA; both D2Rep-2 and D2Rep-1 secreted NS1. Taken collectively, these data indicate that even relatively small levels of codon deoptimization in the same gene lead to lower replication fitness.

3. Discussion

A long-standing challenge in dengue vaccine development is the creation of live attenuated viruses that are replicatively fit enough to elicit a protective (“immunizing”) immune response in vaccine recipients but don’t replicate so much that they elicit clinical signs or symptoms of disease. We describe here a codon deoptimization approach that attenuates the replication of dengue replicons in relevant mammalian cells with a view to developing panels of dengue vaccine candidates.

An attraction of the codon deoptimization approach is that it can be fine-tuned to attain levels of viral replicative attenuation that creates viruses attractive for clinical development. Furthermore, this approach should not be readily susceptible to spontaneous reversion to the parental genotype since the number of mutations can be large (hundreds of base pairs) yet the proteome of the virus is unchanged. Nonetheless, there is still a possibility of compensatory mutations arising during scale-up vaccine production that could result in enhanced protein expression and the emergence of a virus genotype associated with increased virulence. Deoptimization of codon/codon pairs has been deployed to attenuate virus replication [8,10,12,13]. Interestingly, the precise mechanism of reduced replication fitness caused by codon deoptimization remains unclear. The attenuation could be related to the disruption of polyprotein synthesis, its processing, stability, or misfolding. It may be caused by the drastic change of the RNA secondary structure that may affect DENV RNA circularization, RNA-protein interactions and RNA stability.

To study the effects of codon deoptimization in an arbovirus that replicates efficiently in both mosquitoes and mammals, DENV has been previously re-coded to favour the insect codon pair bias [15]. Shifting the encoding preference away from mammals resulted in DENV growing to high titers in insect cells but not in mammalian cells [15]. This is in contrast to our study as we did not optimize DENV to mosquitoes and study if that resulted in DENV growing unfavorably in mammalian cells. Instead we definitively deoptimized DENV to humans to ensure there is virus attenuation. However, another very recent study from the same group complemented our work [18]. They performed codon pair deoptimization of the E, NS3 and NS5 genes in DENV-2 and showed significant reduction of replication as compared to wildtype DENV but they focused on addressing if such recoding could increase DENV replication fitness in its vector, *Aedes aegypti* [18]. Results showed no corresponding increase in fitness in mosquitoes in the DENV variants [18]. Additionally, codon pair deoptimization of the E, NS1 genes of ZIKV to mammals has been performed [19]. Results demonstrated diminished replication fitness in mammalian cells and lesser virulence in a mouse model [19]. Interestingly, ours is the first study that utilized the simpler approach of codon deoptimization, rather than codon pair deoptimization to attenuate DENV. Indeed, it has been recently reported that the codon pair bias does not play a major role in the encoding of viral proteins [20].

Using virus replication (luciferase activity and RNA production) and NS1 secretion as markers of attenuation, our primary observa-

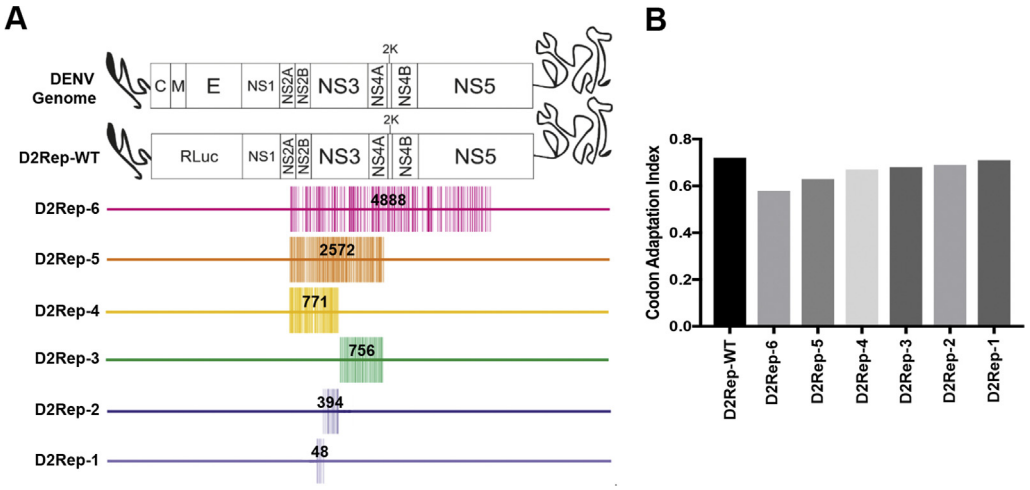

Fig. 1. Representation of the deoptimized constructs with respect to the wildtype DENV-2 replicon and their respective CAI scores. (A) Comparison between the DENV-2 wildtype replicon (D2Rep-WT) and the six constructs with varying degrees and positions of codon deoptimization. The numbers denoted in the coloured section represent the total number of silent mutations in each construct. (B) Graph bar represents the CAI score of the deoptimized replicons. CAI scores are used to measure the amount of codon deoptimization. The formula was first described by Sharp (1987) [23] and calculated by using the http://www.biologicscorp.com/tools/CAICalculator service. CAI score equals to 1 means a maximum efficiency in gene translation in human cells.

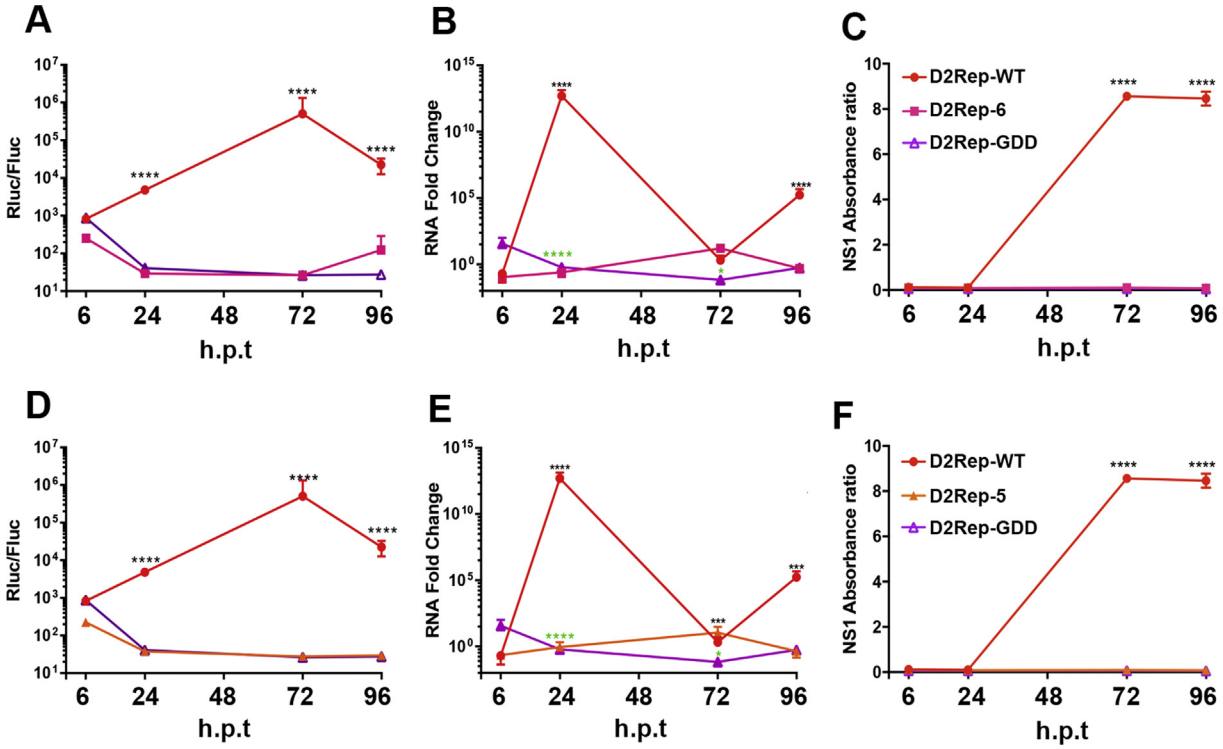

Fig. 2. Extensive codon deoptimization in the DENV-2 replicons abolishes replication. D2Rep-6 RNA with 4888 silent mutations (NS2A-NS5) and D2Rep-5 RNA with 2572 silent mutations (NS2A-NS4A) were transfected into BHK-21 cells. Sampling was performed at 6, 24, 72, and 96 h.p.t. (A, D) Log_{10} luciferase reporter activity (*Rluc*) (y-axis) was normalized to firefly luciferase (*Fluc*) levels as internal normalization controls. (B, E) DENV-2 RNA replication kinetics was analyzed by qRT-PCR and expressed as log_{10} of the level of DENV-2 3′UTR relative to host's GAPDH (C, F) NS1 secretion concentration in cell supernatant measured by DENV NS1 antigen ELISA and expressed as NS1 absorbance/kit standard absorbance ratio. D2Rep-WT: red line; D2Rep-GDD: purple line; D2Rep-6: magenta line; D2Rep-5: orange line. Black asterisks represent statistical significance between the constructs and D2Rep-WT; green asterisks represent statistical significance between the constructs and D2Rep-GDD. Error bars represent the SD of the mean of results of three independent experiments. (For interpretation of the references to colour in this figure legend, the reader is referred to the web version of this article.)

tion in this study is the association between the level of virus attenuation and amount of codon deoptimization. Indeed, replication was completely abolished in constructs D2Rep-6 and D2Rep-5, intermediate with constructs D2Rep-4 and D2Rep-3 and restored almost to wildtype levels with constructs D2Rep-2 and D2Rep-1. Similarly, NS1 secretion is also affected by the level of codon deoptimization. D2Rep-2 secretes significantly lower NS1 as compared to D2Rep-1 which has fewer silent mutations. We found that the position of codon deoptimization within the genome is crucial to the degree of attenuation observed. Despite D2Rep-4 and D2Rep-3 having similar numbers of deoptimized codons, D2Rep-3, which had deoptimized NS3-NS4A, had significantly reduced luciferase

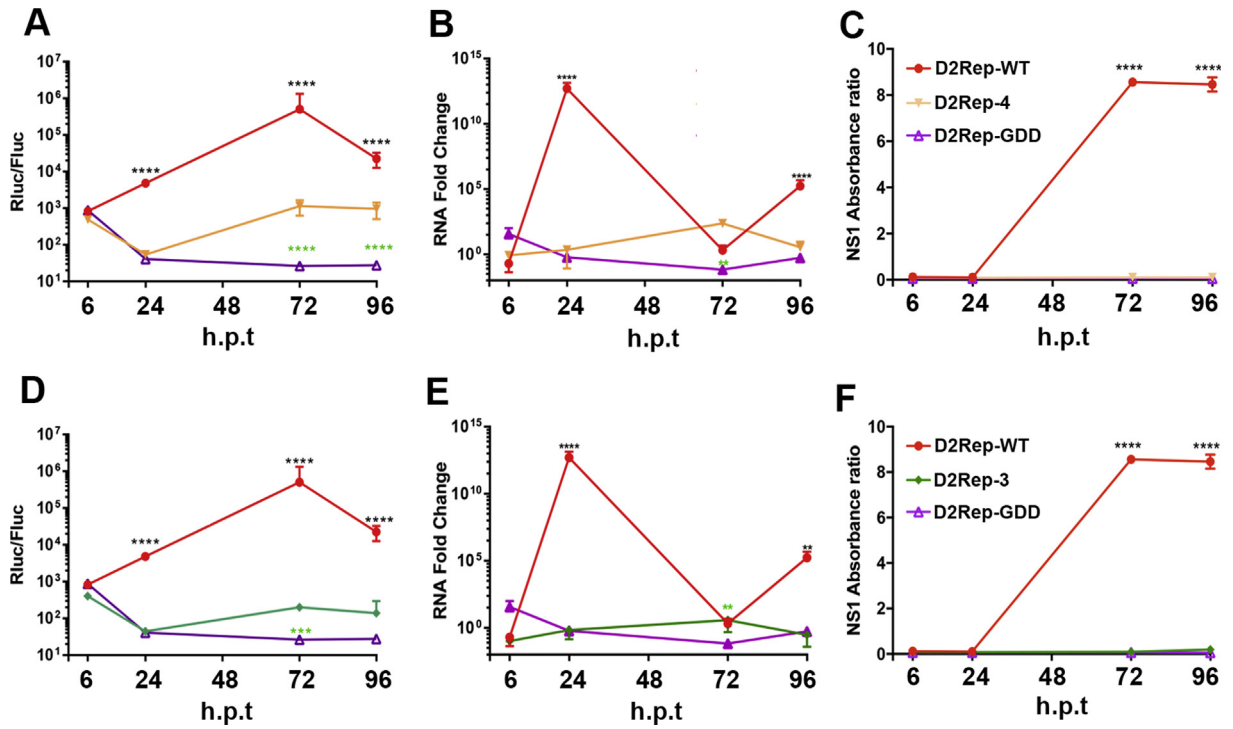

Fig. 3. The location of codon deoptimization in the DENV-2 constructs affects attenuation. D2Rep-4 RNA with 771 silent mutations (NS2A-NS3) and D2Rep-3 RNA with 756 silent mutations (NS3-NS4A) were transfected into BHK-21 cells and sampled at 6, 24, 72, and 96 h.p.t. (A, D) Log_{10} luciferase reporter activity (*Rluc*) (y-axis) was normalized to firefly luciferase (*Fluc*) levels as internal normalization controls. (B, E) DENV-2 RNA replication kinetics was analyzed by qRT-PCR and expressed as log_{10} of the level of DENV-2 3′UTR relative to host's GAPDH (C, F) NS1 secretion concentration in cell supernatant measured by DENV NS1 antigen ELISA and expressed as NS1 absorbance/kit standard absorbance ratio. D2Rep-WT: red line; D2Rep-GDD: purple line; D2Rep-4: yellow line; D2Rep-3: green line. Black asterisks represent statistical significance between the constructs and D2Rep-WT; green asterisks represent statistical significance between the constructs and D2Rep-GDD. Error bars represent the SD of the mean of results of three independent experiments. (For interpretation of the references to colour in this figure legend, the reader is referred to the web version of this article.)

activity in comparison to D2Rep-4, which had deoptimized NS2A-NS3 genes. The lack of difference in RNA levels between both constructs indicates that RNA translation may be more restricted in D2Rep-3 compared to D2Rep-4.

This is the first study that used codon deoptimization as a novel approach to attenuate flavivirus replication for vaccine development. Taken together, our findings indicate that D2Rep-4 and D2Rep-2 display intermediate replication characteristics suitable for possible DENV vaccine candidates. Based on our analysis, we propose that the design for an ideal DENV vaccine candidate could include 394–771 silent mutations within the NS2A and NS3 genes. Indeed, our results, further reinforced by recent studies, suggest that codon deoptimization is an ideal strategy that can readily be used to develop a DENV vaccine candidate with "fine-tuned" attenuation.

4. Materials and methods

4.1. Tissue culture

The baby hamster kidney cell line (BHK-21) was purchased from the American Type Culture Collection (ATCC, USA) and cultured in RPMI 1640 (GibcoTM, Thermo-Fischer, USA) supplemented with 8% fetal calf serum (FCS) (GibcoTM, Thermo-Fischer, USA). The cells were grown in vented flasks at 37 °C with 5% CO_2.

4.2. Cloning of the constructs

The wildtype DENV-2 reporter replicon system (D2Rep-WT) and the replication defective D2Rep-GDD replicon have been previously described and were gifts from Professor Ooi Eng Eong, Singapore [16]. This D2Rep-WT replicon has the backbone of the *Thai 16681* DENV-2 (U87411.1), a well-studied laboratory strain that has formed the basis of a vaccine candidate in clinical trials, and contains *Renilla luciferase* and a T7 promoter region (Fig. 5A) [21,22]. The D2Rep-GDD replicon was designed by replacing the essential GDD motif of the RNA dependent RNA polymerase NS5 in the PD_2Rwt with GVD which makes it completely replication-deficient. A *Firefly luciferase* containing construct (pTNT-*Ffluc*) was used as the normalization control. D2Rep-WT and D2Rep-GDD were transformed into MAX Efficiency® Stbl2TM Competent Cells (Thermo Fisher Scientific, USA) and grown in LB broth supplemented with 100 μg/mL ampicillin (Sigma-Aldrich, USA) overnight at 30 °C. For codon deoptimization, restriction sites within the D2Rep-WT were selected to target the NS genes of DENV-2 genome (Fig. 5B). Then, the six codon deoptimized sequences were ordered from GenScript®, USA. They had been cloned into pUC57 commercial plasmids with corresponding restriction sites at both ends of inserts. They were transformed into MAX EfficiencyTM DH5αTM (Thermo Fisher Scientific, USA). All transformations were carried out using the heat shock method as per manufacturer's instructions. Single colonies were selected and were grown in LB broth supplemented with 100 μg/mL ampicillin (Sigma-Aldrich, USA) overnight at 30 °C. Plasmid DNA was extracted using the Spin miniprep kit (Qiagen, Germany) or the NucleoBond® Xtra Maxi kit (Macherey-Nagel, Germany). DNA concentrations were measured spectrophotometrically by using NanoDropTM 2000 (Thermo Scientific, USA).

Restriction enzyme cloning was used to produce the six deoptimized constructs. D2Rep-WT plasmid served as a vector plasmid and the corresponding pUC57 with codon deoptimized inserts were digested with the same restriction enzyme pairs to create

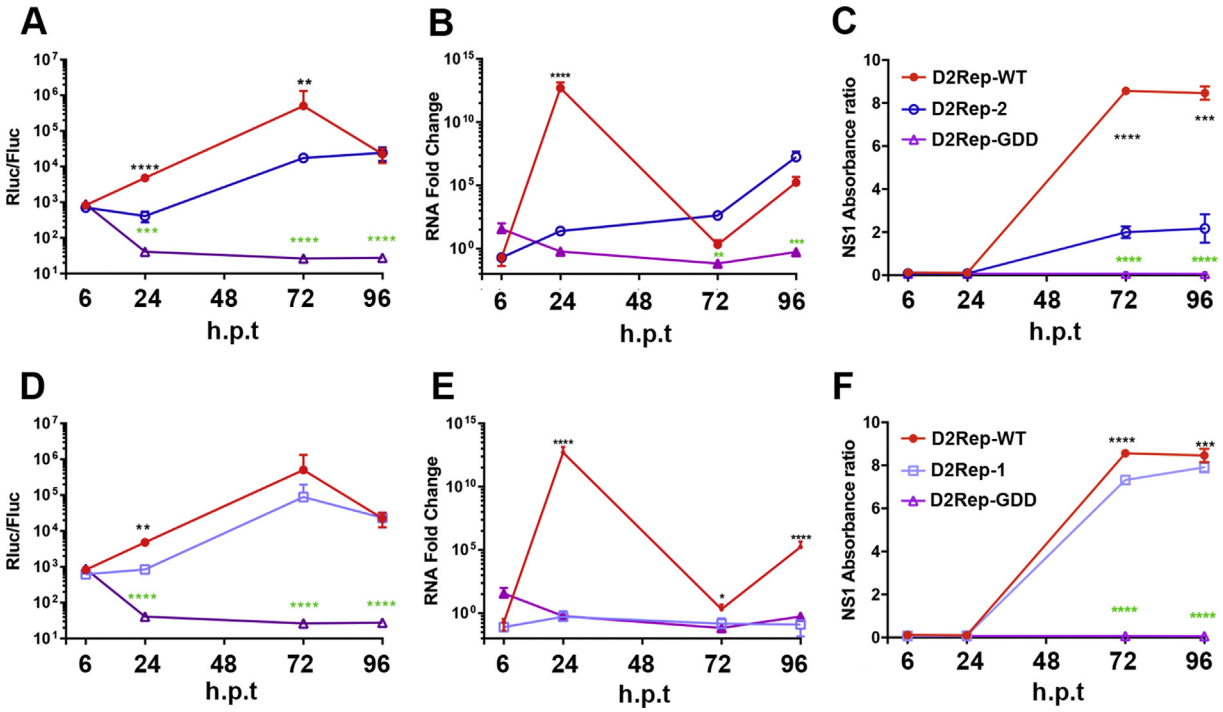

Fig. 4. Small levels of codon optimization in the same gene of the constructs still lead to lower replication fitness. D2Rep-2 RNA with 394 silent mutations and D2Rep-1 RNA with 48 silent mutations in the NS3 gene were transfected into BHK-21 cells and sampled at 6, 24, 72, and 96 h.p.t. (A, D) Log_{10} luciferase reporter activity (*Rluc*) (y-axis) was normalized to firefly luciferase (*Fluc*) levels as internal normalization controls. (B, E) DENV-2 RNA replication kinetics was analyzed by qRT-PCR and expressed as log_{10} of the level of DENV-2 3′UTR relative to host's GAPDH (C, F) NS1 secretion concentration in cell supernatant measured by DENV NS1 antigen ELISA and expressed as NS1 absorbance/kit standard absorbance ratio. D2Rep-WT: red line; D2Rep-GDD: purple line; D2Rep-2: blue line; D2Rep-1: light blue line. Black asterisks represent statistical significance between the constructs and D2Rep-WT; green asterisks represent statistical significance between the constructs and D2Rep-GDD. Error bars represent the SD of the mean of results of three independent experiments. (For interpretation of the references to colour in this figure legend, the reader is referred to the web version of this article.)

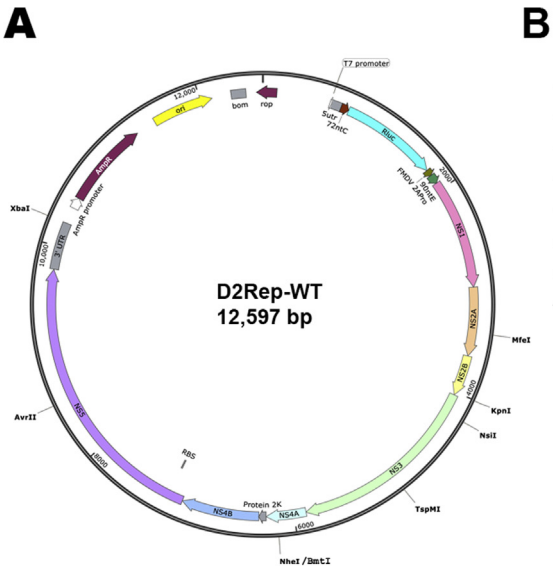

Constructs	Enzyme 1	Enzyme 2
D2Rep-6	MfeI	AvrII
D2Rep-5	MfeI	BmtI
D2Rep-4	MfeI	TspMI
D2Rep-3	TspMI	NheI
D2Rep-2	NsiI	TspMI
D2Rep-1	KpnI	NsiI

Fig. 5. DENV-2 replicon plasmid map (A) D2Rep-WT plasmid with gene segments based on DENV-2 *Thai 16681* strain. The replicon includes a T7 promoter, the 5′UTR, C-terminal 24 amino acids of the C protein for maintaining the topology of protein NS1 within the ER compartment, the renilla luciferase (*Rluc*) fused with a self-cleaving FMDV 2A protease to ensure correct cleavage of the reporter protein and the 30 amino acids of N-terminal E protein followed by the NS genes of DENV-2 strain 16681. (B) Restriction sites used for cloning the deoptimized constructs.

compatible ends. All restriction enzymes were from New England BioLabs® Inc., USA. 5 μg of vectors and inserts were double digested in 1 × CutSmartTM Buffer (New England BioLabs® Inc., USA) with 2 different enzymes at 37 °C for 5 h to ensure complete digestion (Fig. 5B). Following the enzyme digestions, 1 μl of Quick Dephosphorylation Kit (New England BioLabs® Inc., USA) was added to the reaction and incubated for 30 min at 37 °C to prevent recircularization during ligation. Gel electroporation of plasmid digestion products was carried out using 1% agarose gel (Promega, USA) dissolved in 1 × TAE buffer (TP Biomedicals, USA) at 100 V for

60 min. The fragments-of-interest were excised and extracted using QIAquick Gel Extraction Kit (Qiagen, Germany) according to manufacturer's instructions. Following that, the digested products were ligated with the cut D2Rep-WT using the T4 DNA ligase (NEB) at 16 °C overnight and transformed into MAX Efficiency® Stbl2TM Competent Cells (Thermo Fisher Scientific, USA). Colony PCR screenings were done using GoTaq® Flexi DNA polymerase (Promega, USA) to confirm successful cloning. Plasmid sequences were confirmed by sequencing (AGRF, Australia). DNA concentrations were measured spectrophotometrically by using NanoDropTM 2000 (Thermo Scientific, USA).

4.3. In vitro transcription

All plasmid templates were linearized by enzyme digestion using *XbaI* (New England BioLabs® Inc., USA), followed by phenol-chloroform extraction and ethanol precipitation. The *in vitro* transcription to produce capped RNA was carried out by using T7 RiboMAXTM Express Large-Scale RNA Production System (Promega, Madison, USA) with a $m^7G(5')ppp(5')A$ RNA Cap Structure Analog (NEB, USA). The following modifications were used: a total reaction mix of 20 μl was made by mixing 4 μl 5 × buffer, 1.5 μl rGTP, 1.5 μl rCTP, 1.5 μl rUTP, 0.3 μl rATP, 6 μl $m^7G(5')ppp(5')A$ RNA Cap Structure Analog, 2 μl T7 enzyme, 1 μl RNAsin Ribonuclease inhibitor (Promega, Madison, USA), 1 μg linearized DNA template and RNAse-free water. The reaction was incubated at 37 °C, for 30 min. Then, additional 0.6 μl of rATP and 0.15 μl 5 × buffer was added to the reaction. The reaction was then incubated at 37 °C overnight. Following the overnight incubation, 1 μl RNase-Free RQ-DNase (Promega, Madison, USA) was added to the reaction and then incubated for 15 min at 37 °C. RNA yield was then purified using RNeasy® Mini Kit (Qiagen, Germany) and quantified using NanoDropTM 2000 (Thermo Scientific, USA).

4.4. Electroporation

Briefly, BHK-21 cells were trypsinized and washed thrice with cold, sterile PBS after which they were counted and resuspended to 1×10^7 cells/ml in cold Opti-MEM (Invitrogen, USA). 800 μl of the cell suspension was aliquoted into each 4 mm electroporation cuvette (BioRad) followed by addition of 10 μg of purified replicon RNA and 1 μg of pTNT-*Fluc*. After one pulse at 950 μF and 250 V with a Gene Pulser II system (Bio-Rad), cells were incubated at room temperature for 10 min. Cells were gently transferred from each cuvette to 11.2 ml of pre-warmed media and 500 μl of this final mixture was aliquoted into each well (sufficient for a 24-well plate). Cells were harvested at various time-points using the passive lysis buffer (Promega) and luciferase activity was measured using the Dual Luciferase Reporter Assay system (Promega) according to manufacturer's instructions with the CLARIOstar® (BMG Labtech, Germany).

4.5. Quantitative Reverse Transcriptase Polymerase Chain Reaction (qRT-PCR)

Total RNA was extracted from the cellular lysates obtained after addition of the passive lysis buffer from the Dual-Luciferase assay kit (Promega, USA). RNA was purified using RNeasy® Mini Kit (Qiagen, Germany) and quantified using the NanoDropTM 2000 (Thermo Scientific, USA). Superscript III reverse transcriptase and random hexamers (Invitrogen, USA) were used in the reverse transcription reactions to generate cDNA. qRT-PCR was performed. Quantitative real-time PCR (qRT-PCR) was performed on 5 μl of cDNA by using iQ™ SYBR Green Supermix Kit (Biorad, USA) according to manufacturer's instructions. Primers targeted the 3′UTR of DENV-2 genome (LYL For: 5′-TTGAGTAAACYRTGCTGCCTG TAGCTC-3′and LYL-Rev: 5′-GAGACAGCAGGATCTCTGGT-3′) All PCR reactions were done in triplicates and normalized against GAPDH. Reactions were run on the CFX96TM Real-Time System (Biorad, USA). qRT-PCR conditions to detect viral RNA: 95 °C for 5 min, followed by 40 cycles of 95 °C for 10 sec, 55 °C for 5 sec and 72 °C for 10 sec.

4.6. DENV NS1 antigen Enzyme-linked Immunosorbent Assay (ELISA)

Supernatant from electroporated cells were collected at various time-points. The supernatants were then tested for the secretion of NS1 antigen using the Platelia Dengue NS1 Ag (Biorad, USA) according to the manufacturer's protocol. Sample absorbance was measured by using CLARIOstar® (BMG Labtech, Germany).

4.7. Statistical analysis

All results are presented as mean ± SD of at least three independent experiments. Data were analysed using Student's T-Test and considered significant if $p < 0.05$ ($^{*}p < 0.05$; $^{**}p < 0.01$; $^{***}p < 0.001$; $^{****}p < 0.0001$). All calculations were done using GraphPad Prism version 7.0 (GraphPad Software Inc, USA).

Acknowledgements

This work was supported by the Wellcome Trust (UK) and the National Health and Medical Research Council (Australia). The authors wish to thank Professor Ooi Eng Eong, Duke-NUS Medical School, Singapore for providing the dengue 2 replicon used in this study.

Conflict of interest

The authors declare no conflicts of interest.

Appendix A. Supplementary material

Supplementary data to this article can be found online at https://doi.org/10.1016/j.vaccine.2019.03.062.

References

[1] Bhatt S, Gething PW, Brady OJ, Messina JP, Farlow AW, Moyes CL, et al. The global distribution and burden of dengue. Nature 2013;496:504–7.
[2] Villar L, Dayan GH, Arredondo-Garcia JL, Rivera DM, Cunha R, Deseda C, et al. Efficacy of a tetravalent dengue vaccine in children in Latin America. N Engl J Med 2015;372:113–23.
[3] Capeding MR, Tran NH, Hadinegoro SR, Ismail HI, Chotpitayasunondh T, Chua MN, et al. Clinical efficacy and safety of a novel tetravalent dengue vaccine in healthy children in Asia: a phase 3, randomised, observer-masked, placebo-controlled trial. Lancet 2014;384:1358–65.
[4] Grantham R, Gautier C, Gouy M, Mercier R, Pave A. Codon catalog usage and the genome hypothesis. Nucleic Acids Res 1980;8:r49–62.
[5] Gustafsson C, Govindarajan S, Minshull J. Codon bias and heterologous protein expression. Trends Biotechnol 2004;22:346–53.
[6] Jenkins GM, Rambaut A, Pybus OG, Holmes EC. Rates of molecular evolution in RNA viruses: a quantitative phylogenetic analysis. J Mol Evol 2002;54:156–65.
[7] Woelk CH, Holmes EC. Reduced positive selection in vector-borne RNA viruses. Mol Biol Evol 2002;19:2333–6.
[8] Coleman JR, Papamichail D, Skiena S, Futcher B, Wimmer E, Mueller S. Virus attenuation by genome-scale changes in codon pair bias. Science 2008;320:1784–7.
[9] Gutman GA, Hatfield GW. Nonrandom utilization of codon pairs in Escherichia coli. Proc Natl Acad Sci USA 1989;86:3699–703.
[10] Mueller S, Papamichail D, Coleman JR, Skiena S, Wimmer E. Reduction of the rate of poliovirus protein synthesis through large-scale codon deoptimization causes attenuation of viral virulence by lowering specific infectivity. J Virol 2006;80:9687–96.
[11] Broadbent AJ, Santos CP, Anafu A, Wimmer E, Mueller S, Subbarao K. Evaluation of the attenuation, immunogenicity, and efficacy of a live virus vaccine generated by codon-pair bias de-optimization of the 2009 pandemic H1N1 influenza virus, in ferrets. Vaccine 2016;34:563–70.

[12] Cheng BY, Ortiz-Riano E, Nogales A, de la Torre JC, Martinez-Sobrido L. Development of live-attenuated arenavirus vaccines based on codon deoptimization. J Virol 2015;89:3523–33.
[13] Cheng BYH, Nogales A, de la Torre JC, Martinez-Sobrido L. Development of live-attenuated arenavirus vaccines based on codon deoptimization of the viral glycoprotein. Virology 2017;501:35–46.
[14] Le Nouen C, Brock LG, Luongo C, McCarty T, Yang L, Mehedi M, et al. Attenuation of human respiratory syncytial virus by genome-scale codon-pair deoptimization. Proc Natl Acad Sci USA 2014;111:13169–74.
[15] Shen SH, Stauft CB, Gorbatsevych O, Song Y, Ward CB, Yurovsky A, et al. Large-scale recoding of an arbovirus genome to rebalance its insect versus mammalian preference. Proc Natl Acad Sci USA 2015;112:4749–54.
[16] Holden KL, Stein DA, Pierson TC, Ahmed AA, Clyde K, Iversen PL, et al. Inhibition of dengue virus translation and RNA synthesis by a morpholino oligomer targeted to the top of the terminal 3' stem-loop structure. Virology 2006;344:439–52.
[17] Carbone A, Zinovyev A, Kepes F. Codon adaptation index as a measure of dominating codon bias. Bioinformatics 2003;19:2005–15.
[18] Stauft CB, Shen SH, Song Y, Gorbatsevych O, Asare E, Futcher B, et al. Extensive recoding of dengue virus type 2 specifically reduces replication in primate cells without gain-of-function in Aedes aegypti mosquitoes. PLoS One 2018;13:e0198303.
[19] Li P, Ke X, Wang T, Tan Z, Luo D, Miao Y, et al. Zika virus attenuation by codon pair deoptimization induces sterilizing immunity in mouse models. J Virol 2018;92.
[20] Kunec D, Osterrieder N. Codon pair bias is a direct consequence of dinucleotide bias. Cell Rep 2016;14:55–67.
[21] Butrapet S, Huang CY, Pierro DJ, Bhamarapravati N, Gubler DJ, Kinney RM. Attenuation markers of a candidate dengue type 2 vaccine virus, strain 16681 (PDK-53), are defined by mutations in the 5' noncoding region and nonstructural proteins 1 and 3. J Virol 2000;74:3011–9.
[22] Kinney RM, Butrapet S, Chang GJ, Tsuchiya KR, Roehrig JT, Bhamarapravati N, et al. Construction of infectious cDNA clones for dengue 2 virus: strain 16681 and its attenuated vaccine derivative, strain PDK-53. Virology 1997;230:300–8.
[23] Sharp PM, Li WH. The codon Adaptation Index–a measure of directional synonymous codon usage bias, and its potential applications. Nucleic Acids Res 1987;15:1281–95.